ISSN 1063-7842, Technical Physics, 2018, Vol. 63, No. 2, pp. 250–256. © Pleiades Publishing, Ltd., 2018.
Original Russian Text © O.G. Fedotov, V.M. Fomin, 2018, published in Zhurnal Tekhnicheskoi Fiziki, 2018, Vol. 63, No. 2, pp. 258–264.

OPTICS

Prospects for Practical Applications of a Discharge Chemical HF Laser as a Coherent Source for IR Holography

O. G. Fedotov and V. M. Fomin*

Institute of Electrophysical Devices,
St. Petersburg, 196641 Russia

**e-mail: vitfominm@gmail.com*

Received April 3, 2017; in final form, July 23, 2017

Abstract—Preliminary experimental results on recording of phase and amplitude holograms using the radiation of electric-discharge HF lasers are presented, and prospects for applications of such lasers in diagnostics of various objects are discussed. It is shown that lasers with homogeneous working medium may generate coherent radiation with a coherence length of greater than 6 m in the absence of mode selection. Methods for control of spatial distribution of electron concentration in excimer and discharge chemical HF (DF) lasers and distributions of the main combustible components are considered. Deposition of holographic identification marks on artworks is studied.

DOI: 10.1134/S1063784218020135

INTRODUCTION

It is known from [1, 2] that IR lasers may be superior to visible-range lasers in holographic diagnostics of plasma owing to the fact that the detection sensitivity of electron concentration is proportional to the radiation wavelength whereas the sensitivity of interference pattern with respect to density gradient of neutral particles is inversely proportional to the wavelength. Thus, the interference diagnostics of plasma objects in the mid-IR range can be performed with negligibly low measurement error of the distribution of electron concentration related to the density gradient of heavy particles. The minimum detectable product of electron concentration N_e and length of plasma object L can be calculated as [2]

$$(N_eL)_{\min} \approx 2.2\times10^{13}k_{\min}/(C_s\lambda)\ \text{cm}^{-2}, \qquad (1)$$

where λ is the radiation wavelength, $k_{\min}$ is the minimum detectable shift of interference fringe (normally, 0.1 of the fringe width), and C_s is the sensitivity coefficient.

The sensitivity coefficient is proportional to the number of passages of radiation through the object under study and the nonlinearity of hologram. The measurement sensitivity of electron concentration increases by a factor of $2n$ when the holograms are reconstructed in the $\pm n$ diffraction orders [2].

Efficient diagnostics of the distribution of electron concentration using CO_2 lasers has been shown for various plasma objects (see [1, 2] and references therein). In diagnostics of arc discharges, nonlinear holograms can be recorded and reconstructed using up to seven diffraction orders and a scheme for compensation of aberrations that increase with an increase in the diffraction order can be implemented.

Modern CO_2 lasers are employed for diagnostics of plasma [3, 4] and interferometric monitoring of the shape and deformation of various objects, in particular, large-size mirrors [5], building structures [6], and artworks [7]. In the last case, an interferogram in which hidden defects of an artwork are recorded can be stored in computer media and may serve as an individual identification mark that may prevent substitution of a copy for original artwork.

Electric-discharge nonchain HF chemical lasers were used for diagnostics of plasma in the 1970s [8, 9]. Distributions of electron concentration in the discharge plasma in the Z- and θ-pinch configurations have been measured. Holograms have been recorded in gelatin and bismuth films. An interference pattern with a spatial frequency of 300 mm^{-1} can be recoded in gelatin at an irradiation flux of 2 J/cm^2 [8]. At a flux of 0.5–1.0 J/cm^2, the resolution for a bismuth film is no worse than 500 mm^{-1} and the threshold flux for recording is no greater than 0.1 J/cm^2 [9].

Nonselective lasing has been employed in [8] in the study of the θ-pinch discharge in a cylindrical quartz vessel. A superposition of 5–8 phase holograms has been recorded. Sequential reconstruction of such holograms makes it possible to decrease the error of determination of electron concentration. The minimum measured product N_eL was 10^{16} cm^{-2}. Single-line lasing has been used in [9] to record amplitude

holograms with a minimum product $N_e L$ of 8×10^{15} cm^{-2}.

The holographic method can also be employed in the measurement of the spatial distribution of the spectral composition of the HF-laser radiation and the dependence of the radiation spectrum on the initial pressure of the gas mixture [10].

Evidently, CO_2 lasers are superior to HF lasers with respect to the measurement sensitivity of electron concentration. However, the latter exhibit several advantages. In particular, the radiation of HF lasers is transmitted with minor loss by the walls of quartz vessels in which various plasma structures are formed, walls of xenon and exciplex lamps, and output and diagnostic windows that are transparent in the visible and UV spectral ranges.

Note the absence of progress in the holographic diagnostics of plasma with the aid of HF lasers related to the absence of convenient recording media with relatively low recording thresholds and, hence, application of lasers with relatively high output energy. Such lasers have been cumbersome and complicated. In particular, holograms have been recorded on gelatin films with the aid of a laser with multipoint (2000) cathode, a discharge chamber length of 3 m, and an output energy of 10 J [8]. An oscillator–amplifier system with the selection of transverse modes, an output energy of 2.5 J, and an efficiency of about 0.2% has been used for hologram recording on bismuth films [9].

In this work, we present preliminary results on the recording of holograms with the aid of discharge HF lasers with output energies of 0.07–1.5 J. We also discuss prospects for application of the HF (DF) lasers in the diagnostics of plasma, in particular, the study of plasmachemical kinetics of excimer and chemical lasers.

EXPERIMENTAL SETUP

In the experiments, we use two laser setups that have been constructed at the Institute of Electrophysical Devices.

In the first setup, the volume discharge is formed in a mixture of sulfur hexafluoride and hydrogen due to the X-ray preionization using the radiation of creeping discharge [11]. Such a discharge is formed on the walls of the discharge chamber (fluoroplastic tube with an inner diameter of 100 mm) in the presence of a voltage pulse (with an amplitude of up to 400 kV, a duration of 50 ns, and a leading edge of less than 10 ns) across the interelectrode gap. A specific feature of the system for the generation of the volume discharge is the simultaneous formation of the creeping and volume discharges in a single interelectrode gap. The creeping discharge is generated at a relatively high rate of an increase in the voltage across the interelectrode gap that is sufficient for the generation of the runaway electrons and emission of soft X-rays [12]. A decrease in the voltage across the discharge gap related to the formation of the volume discharge leads to a decrease in the ionization rate in the creeping discharge layer and prevents the transition of plasma of the creeping discharge to high-conductivity state at a sufficiently small duration of the applied voltage.

Windows made of calcium fluoride (fluorite) are mounted on the ends of the discharge chamber and orthogonally oriented to the optical axis. In the original variant of [11], the laser electrodes with a width of the plane part of 6 cm and a length of 50 cm are placed at a distance of 6 cm from each other. The transverse size of the laser beam is 6×6 cm. However, the distribution of the laser energy density in such a laser is nonmonotonic and has a minimum at the symmetry axis.

In this work, we use the laser setup in which segment-cylindrical electrodes with a curvature radius of 5 cm are placed in the discharge chamber. The applied voltage is decreased to a level of 250 kV. Figure 1 shows the schematic drawing of the discharge chamber and the photograph of the volume-discharge plasma at a sulfur hexafluoride pressure of 10 kPa.

The cavity with a length of 1 m consists of plane mirrors. The totally reflecting mirror has aluminum coating, and the output mirror has a reflectance of about 50% in the laser spectral band (2.6–3.0 μm).

In preliminary experiments, we have studied the conditions for generation of uniform volume discharge in the laser with the X-ray preionization. A holographic setup based on the OGM-20 ruby laser [13] have been used to monitor the optical density distribution of the volume discharge. Figure 2 presents typical interferograms of the volume and creeping discharges. For the visualization of the creeping discharge, the optical axis of the holographic setup has been moved upwards by 10 mm (Figs. 2c and 2d), since the aperture of the probe beam (about 90 mm) has been less than the inner diameter of the discharge chamber.

The laser active medium is relatively homogeneous in the working regime at a pressure of the gas mixture ($SF_6 : H_2 = 12 : 1$) of 5–15 kPa. Substantial perturbations of the gas mixture are observed only after the termination of lasing. The sizes of the region of the volume discharge are $1.6 \times 6 \times 50$ cm, the laser energy is 1.5 J, and the laser pulse duration is 150 ns. Laser spark in air that is observed when the radiation is focused using a spherical lens with a focal length of 160 mm proves relatively high optical quality of the active medium.

In this work, we also use a FLIP-1 discharge laser, which is the first Russian repetitively pulsed chemical laser with the closed gas-dynamic contour [14].

Preliminary changes of the electrode unit and initiation system of the laser of [14] make it possible to increase the width of the region of the discharge plasma and uniformity of the distribution of energy deposition to the volume discharge. Thus, the laser efficiency can be increased to 3% at a charging voltage

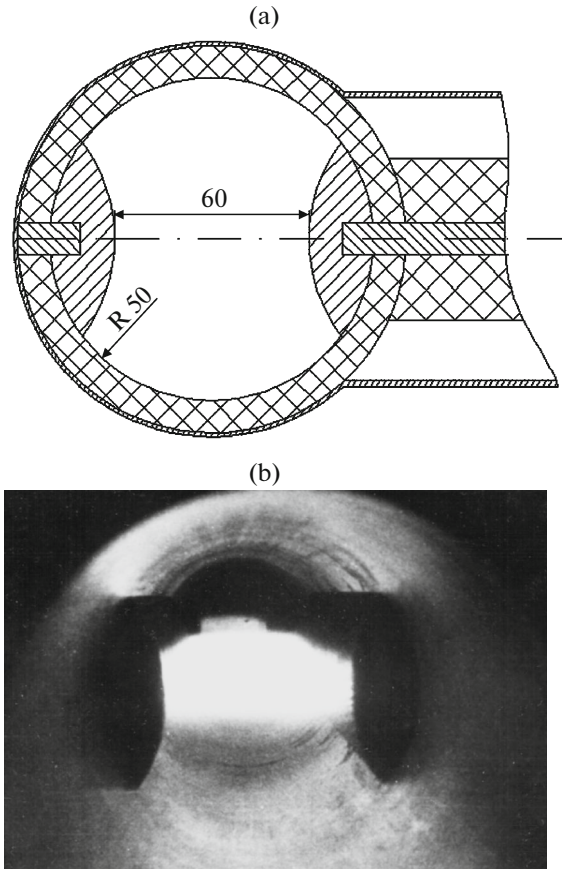

Fig. 1. (a) Schematic drawing of the discharge chamber and (b) photograph of the discharge gap.

of 25 kV and an activation energy per pulse of 85 mJ. The volume discharge with a duration of about 100 ns is formed using the UV preionization with the aid of multispark discharge in the circuit of peaking capacitor. The length of the plane part of electrodes is 30 cm, the interelectrode distance is 14 mm, and the width of the discharge region is close to the width of the interelectrode gap (16 mm). The duration of the laser pulse is about 100 ns at a ratio of the gas-mixture components of $SF_6 : H_2 = 6 : 1$.

In both lasers, the laser pulse duration can easily be decreased to 50 ns due to an increase in hydrogen content in the gas mixture.

Figure 3 presents the simplified schemes for the hologram recording. The output beam is split into the reference and object beams using germanium plate BS. The difference of the optical path lengths of the beams ranges from 1 to 6.5 m. Phase and amplitude holograms are recorded in the experiments.

For the recording of the phase holograms, the beams are focused by fluorite lenses $L1$ and $L2$ on gelatin film H that covers exposed photographic film (photoplate) or film of bleached linseed oil deposited on a fluorite film (linseed oil is widely used in art for deposition of protecting coating).

For recording of amplitude holograms, the beams are directed to an FPGV-2 photoplate sensitized for the radiation wavelength of the ruby laser. In this case, the recording is performed using the thermal sensitization (see, for example, [15]) when the IR radiation generates thermal relief on the surface of photoplate and the image of such relief is formed due to the photochemical effect of visible radiation (e.g., radiation of xenon flash lamp).

In this work, the OGM-20 ruby laser (that has been employed for holographic diagnostics of the uniformity of volume discharge) serves as a source of actinic light. The radiation of the ruby laser having passed through diffusion scatterer S is used to irradiate the film from the rear side. The illuminating laser works in the Q-switching regime, and the duration of the laser pulse is about 100 ns. The time interval between the pulses of the chemical and ruby lasers ranges from 0.1 to 10 μs. To prevent incoherent illumination of the photographic film, we use germanium filters $F1$ and $F2$ and the KS-18 glass filter.

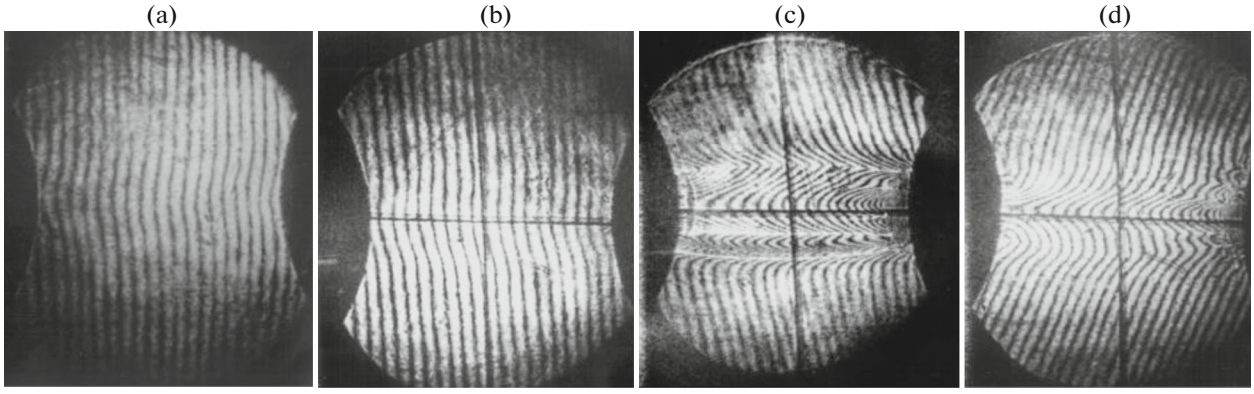

Fig. 2. Interferograms of the volume discharge in SF_6 that are measured with delays of (a) 0.28, (b) 0.7, (c) 20, and (d) 15 μs at sulfur fluoride pressures of (a–c) 10 and (d) 5 kPa and applied voltages of (a–c) 250 and (d) 210 kV.

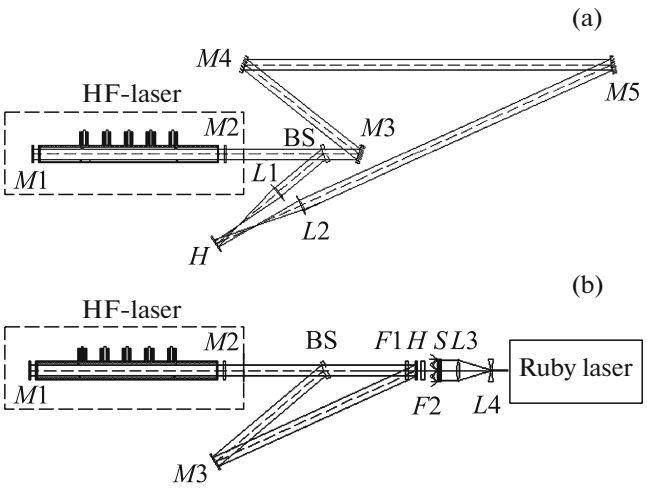

Fig. 3. Experimental optical schemes for recording of (a) phase and (b) amplitude holograms: $M1$–$M5$ plane mirrors, $L1$–$L4$ lenses, $F1$ and $F2$ optical filters, BS germanium beamsplitter, S diffuser, and H detector.

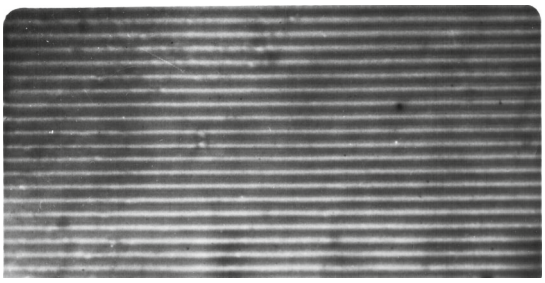

Fig. 4. Fragment of the magnified image of the phase hologram on the gelatin film.

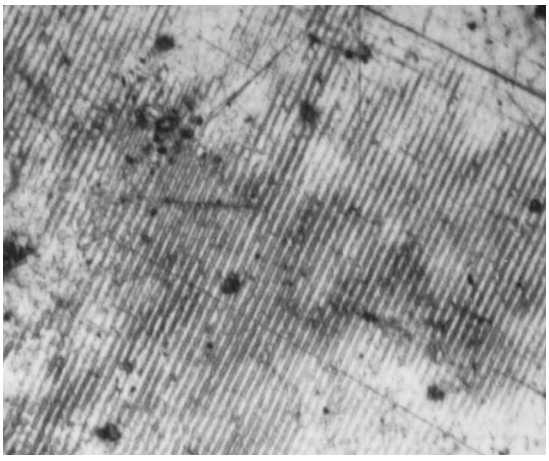

Fig. 5. Fragment of the magnified image of the diffraction grating on the surface of the linseed-oil film.

EXPERIMENTAL RESULTS AND DISCUSSION

Figure 4 presents a fragment of the magnified image of the phase hologram. Phase holograms are recorded due to changes of the surface relief of the gelatin film induced by high-power laser radiation. Nonlinear holograms are reconstructed with a relatively high quality in the ±6th diffraction orders, which makes it possible to increase the measurement sensitivity of quantity N_eL by a factor of 12 [1, 2]. At a laser fluence of about 0.5 J/cm^2, the spatial frequency of the recorded gratings ranges from 100 to 140 mm^{-1} and corresponds to the difference of the angles of incidence of laser beams. In this case, the dynamic range is no less than 3 and the diffraction efficiency in the ±1st orders (about 10%) is sufficiently uniform over the image field. When the difference of the optical path lengths is increased to 6.5 m, the diffraction efficiency remains almost unchanged. For comparison, note that the coherence length of the erbium laser [15] with a radiation wavelength of $\lambda = 2.94$ μm is only 3.3 cm.

The diffraction efficiency of the amplitude holograms at fluences of 0.1 J/cm^2 is significantly lower (about 1%). The spatial frequency of the recorded grating is about 120 mm^{-1}. At a time interval of 10 μs between the pulses of the chemical and illuminating lasers, the diffraction efficiency remains almost unchanged.

The radiation of the FLIP-1 laser with a pulse energy of 60 mJ is divided into two beams with almost identical intensities and a difference of the path lengths of no greater than 1 m. Such beams are used to record diffraction gratings in several materials (gelatin, metallized lavsan, and dried linseed oil). A diffraction grating is recorded on the linseed-oil film deposited on a fluorite plate at a fluence of about 1 J/cm^2. Figure 5 shows a fragment of the magnified image of the surface of the lacquer film. With a delay of 10 years relative to recording, the illumination of the exposed sample using the radiation of the He–Ne laser yields splitting of the transmitted (and reflected) beams into seven beams. A colored spot is observed in the transmitted and reflected beams at certain angles when the hologram is illuminated using sunlight.

Such a result can be used in the study aimed at the application of the HF lasers in the art security encoding.

The irradiation of the gelatin layer of the photographic film and metallized lavsan makes it possible to obtain structures that provide splitting of the reflected beam of the He–Ne laser into five and three beams, respectively. Note that the volume discharge in the FLIP-1 laser is less uniform in comparison with the discharge in the laser with the X-ray preionization. Single streams with diameters of 4–5 mm are observed in the discharge structure.

The results prove relatively high coherence of radiation for the discharge chemical lasers with uniform initiation of the volume discharge in the absence of the mode selection.

The measurement sensitivity of the electron concentration in plasma diagnostics using HF lasers is higher than the sensitivity provided by the ruby laser by a factor of 40.

The results of this work characterize coherent characteristics of nonchain chemical lasers based on hydrogen fluoride. In our opinion, a transition to the generation using deuterium fluoride ($\lambda = 3.4$–4 μm) will not lead to noticeable variations in the coherence of radiation.

Based on the absorption spectra of normal [16] and deuterated [17] gelatin and the experimental results of [15], we conclude that the threshold fluence needed for the recoding of holograms with the aid of thermal sensitization is no greater than 1 mJ/cm^2 for both HF and DF lasers.

Practical implementation of the holographic recording using the radiation of the DF laser will make it possible to increase the sensitivity of the electron concentration measurement and solve new problems.

PROSPECTS FOR APPLICATION

The prospects for application of the HF and DF lasers as radiation sources of interferometric diagnostic setups must be analyzed with allowance for specific features of the above experimental setup including disadvantages related to complicated structure and operation.

Progress in the development of systems for initiation of discharge chemical lasers [18–21] and cold-cathode thyratrons [22] stimulates the development of a commercially available HF (HD) laser with a relatively low repletion rate, closed gas-dynamic system including purification system [14], and an output energy of 1–2 J.

In our opinion, a laser with the resistive stabilization of the volume discharge using solid electrodes made of titanium-containing ceramic material doped with niobium is the optimal laser for a holographic setup. Such an electrode system for the stabilization of the volume discharge that has been proposed in [23] is a reliable and efficient system for initiation of repetitively pulsed chain and nonchain HF (HD) lasers [21].

Efficient application of the HF and DF lasers in the holographic recording is possible due to availability of noncooled photodetector arrays with relatively high sensitivity in the spectral interval of the lasers. In particular, an Ophir Optronics PIROCAM IV camera makes it possible to record interferograms with sizes of 2.54 × 2.54 cm, a resolution of 80 μm, a sensitivity of 10 μJ/cm^2, and a dynamic range of 1000.

Fast pulsed LEDs may serve as sources of actinic light for the recording of holograms with the aid of thermal sensitization.

In our opinion, high-coherence HF (DF) lasers can be used to solve several topical problems.

Long-pulse excimer and discharge chemical lasers are plasma objects that can be studied with the aid of the HF and DF lasers.

In the XeCl excimer lasers, the electron concentration may amount to 10^{15}–10^{16} cm^{-3} [24–26]. When the discharge gap is relatively long, quantity N_eL is sufficient for the holographic diagnostics of the transverse distribution of electron concentration in the interelectrode gap if a ruby laser serves as the radiation source. In particular, a shift of the interference fringes by 0.75 at the maximum current and the formation of the cathode–anode channels were observed in the measurements of electron concentrations of up to 3×10^{15} cm^{-3} in the discharge gap with a length of 80 cm using a ruby laser [26]. In diagnostics of the XeCl laser using the probe radiation of the HF laser and reconstruction of holograms in the first diffraction order, the shift was more than 3 fringes and the diagnostic accuracy with respect to electron concentration was higher by a factor of 4 [26].

The recording of nonlinear holograms makes it possible to visualize electron distributions both across and along electrodes and in the vicinity of the edges of electrodes (regions that are important for discharge stability and formation of directional pattern). In particular, the shift at the maximum current is about one fringe when the diagnostics of the laser of [26] is performed using the reconstruction of nonlinear hologram in the fourth diffraction order.

Evidently, holographic methods can be used in diagnostics of the KrF (and alternative excimer) lasers that wok in the long-pulse regime with a duration of the current pulse of greater than 100 ns.

In the discharge chemical lasers, the electron concentration at the maximum current may amount to 2×10^{14} cm^{-3} in accordance with the calculations of [27, 28] and the reduced surface density of electrons may reach a level of $N_eL = 10^{16}$ cm^{-2} [28, 29]. A linear hologram can be recorded using two passages of the radiation of the DF laser ($\lambda \approx 3.8$ μm) through the active medium of the HF laser [29] and the shift at the maximum current is about 0.33 fringes.

It is known from [2] that a linear hologram depends on both phase and amplitude distortions of the object wave. The holographic method is insensitive to the natural radiation of plasma (active medium of laser), which is incoherent radiation that is not involved in the formation of the interference structure of the hologram. Relatively high accuracy of the measurement of absorption coefficient using the holographic method has been shown in [30]. Thus, it is expedient to employ DF lasers in monitoring of concentrations of combustible components of gas mixtures of discharge lasers, in particular, hydrogen chloride in excimer (XeCl, KrCl, and ArCl) lasers and saturated hydrocarbons (C_2H_6, C_3H_8, and C_4H_{10}) in chemical HF lasers.

It is known from [31] that the $2P(3)$ radiation of the DF laser is strongly absorbed by the HCl molecules. The results of [25] show that a decrease in the content of such a component of the laser mixture may amount to 90% at the moment of termination of current flow in the discharge gap. The reduced absorption coefficient of hydrogen chloride in nitrogen at atmospheric pressure is relatively high (greater than 5 m^{-1} kPa^{-1}) [31]. The initial partial pressure of hydrogen chloride in the mixtures of the XeCl lasers ranges from 0.1 to 1 kPa, so that the absorption coefficient per single passage is ~0.3–0.97 for a typical electrode length of about 70 cm. The measurement accuracy for relatively high concentrations of HCl can be increased for the $P2(4)$ generation, since the corresponding absorption coefficients are lower (0.015 m^{-1} kPa^{-1}) [31]. Relatively high absorbance for the $2P(3)$ radiation can be used to monitor spatial structure of the combustion of HCl both across and along the optical axis of the laser setup.

The absorption coefficients of the C_2H_6, C_3H_8, and C_4H_{10} molecules (that are used as donors of hydrogen in the nonchain HF lasers) at the generation lines of the DF lasers are 0.1–0.2 m^{-1} kPa^{-1} [32]. Our estimations yield combustion of about 50% for donors of hydrogen at a typical pressure of hydrocarbons of about 0.5 kPa. Thus, the determination of the combustion field for such substances is a complicated metrological and phenomenological problem that, however, can be solved with the aid of the holographic methods. Such methods make it possible to eliminate the effect of stray light of the active medium and to employ procedures related to variations in the threshold fluence needed for hologram recording (the fluence at the maximum of interference fringe in the unperturbed medium must be less than the threshold level). The sensitivity of the method and the accuracy of concentration measurements for donors of hydrogen can be increased using a system with additional cuvette in the reference beam (the content of hydrocarbons in such a cuvette must be varied in the desired intervals).

In addition to pulsed discharge excimer and chemical lasers, we can study repetitively pulsed and cw chain chemical HF (DF) lasers. The holographic methods can be used to visualize distributions of the HF and DF molecules in the active medium of such lasers.

Note also topicality of the determination of the distribution of electron concentration in the plasma of xenon lamps that are used for laser pumping.

HF lasers can be used for fabrication of holographic identification marks on paintings that prevent substitutions. Excimer lasers are employed at present for recording of computer generated holograms on the surface of paintings [33].

CONCLUSIONS

Preliminary results of this work must be specified. First, we must determine threshold exposures and sensitivities of holographic recording on different materials using HF and DF laser lines.

Note that recording and reconstruction of holograms (especially, nonlinear) are complicated experimental problems but the measurements of spatial distributions of electron concentrations and combustible components of excimer and chemical lasers will make it possible to substantially improve reliability and predictive power of mathematical models that are used for calculation of characteristics of such lasers.

ACKNOWLEDGMENTS

This work had been initiated and supervised by V.G. Smirnov and is devoted to his memory.

REFERENCES

1. A. N. Zaidel', G. V. Ostrovskaya, and Yu. I. Ostrovskii, Zh. Tekh. Fiz. **38**, 1405 (1968).
2. G. V. Ostrovskaya, Tech. Phys. **53**, 1103 (2008).
3. P. Acedo, H. Lamela, M. Sanchez, T. Estrada, and J. Sanchez, Rev. Sci. Instrum. **75**, 4671 (2004).
4. C. E. Thomas, L. R. Baylor, Jr., S. K. Combs, S. J. Meitner, D. A. Rasmussen, E. M. Granstedt, R. P. Majeski, and R. Kaita, Rev. Sci. Instrum. **81**, 527 (2010).
5. M. P. Georges, J. F. Vandenrijt, C. Thizy, Y. Stockman, P. Queeckers, F. Dubois, and D. Doyle, Appl. Opt. **52**, 102 (2013).
6. I. Alexeenko, J. F. Vandenrijt, M. Georges, G. Pedrini, T. Cedric, W. Osten, and B. Vollheim, Appl. Mech. Mater. **24–25**, 147 (2010).
7. V. Tornari, E. Bernikola, W. Osten, R. M. Groves, G. Marc, G. M. Hustinx, and S. Hackney, Proc. SPIE **6618**, 715 (2007).
8. W. Braun, Phys. Lett. A **47**, 144 (1974).
9. R. Kristal, Appl. Opt. **14**, 628 (1975).
10. W. W. Braun, Opt. Eng. **14**, 208 (1975).
11. V. A. Burtsev, V. M. Vodovozov, P. N. Dashuk, S. L. Kulakov, V. F. Prokopenko, V. M. Fomin, and L. L. Chelnokov, in *Proc. II All-Union Conf. on the Physics of Electrical Breakdown of Gases, Tartu, 1984*, p. 414.
12. P. N. Dashuk and S. L. Kulakov, Pis'ma Zh. Tekh. Fiz. **7**, 853 (1981).
13. V. A. Burtsev, L. A. Zelenov, I. L. Kamardin, R. F. Kurunov, A. A. Kuchinskii, V. K. Ratkevich, V. A. Rodichkin, V. G. Smirnov, and B. F. Shanskii, Sov. J. Quantum Electron. **18**, 107 (1988).
14. V. A. Burtsev, M. V. Bezgreshnov, K. I. Finkel'shtein, and V. M. Fomin, in *Proc. All-Union Conf. "Physics and Conversion," Kaliningrad, 1991*, p. 161.
15. T. N. Vadkovskaya, Yu. A. Drozhbin, V. A. Lobachev, T. M. Murina, A. M. Prokhorov, and V. V. Trofimenko, Sov. J. Quantum Electron. **18**, 144 (1988).
16. L. A. Kartuzhanskii, I. F. Mishunin, and V. A. Tsentrovskii, Ukr. Fiz. Zh. **23**, 267 (1978).

17. T. B. Gorlin, L. G. Paritskii, and T. V. Tisnek, Zh. Tekh. Fiz. **57**, 159 (1987).
18. V. V. Apollonov, S. Yu. Kazantsev, V. F. Oreshkin, and K. N. Firsov, Quantum Electron. **28**, 116 (1998).
19. V. D. Bulaev, V. S. Gusev, S. Yu. Kazantsev, I. G. Kononov, S. L. Lysenko, Yu. B. Morozov, A. N. Poznyshev, and K. N. Firsov, Quantum Electron. **40**, 615 (2010).
20. A. N. Panchenko and V. F. Tarasenko, Tech. Phys. Lett. **30**, 454 (2004).
21. E. A. Klimuk, K. A. Kutumov, and G. A. Troshchinenko, Quantum Electron. **40**, 103 (2010).
22. V. D. Bochkov, S. Yu. Kazantsev, I. G. Kononov, and S. V. Podlesnikh, in *Proc. VIII Int. Conf. on Plasma Physics and Plasma Technology, Minsk, 2015*, Vol. 2, p. 459.
23. E. P. Bel'kov, P. N. Dashuk, G. L. Spichkin, and V. M. Fomin, Pis'ma Zh. Tekh. Fiz. **12**, 278 (1986).
24. A. V. Eletskii, Sov. Phys. Usp. **21**, 502 (1978).
25. Yu. I. Bychkov, S. A. Yampol'skaya, and A. G. Yastremskii, Quantum Electron. **40**, 28 (2010).
26. A. De Angelis, P. Lazzaro, F. Garosi, G. Giordano, and T. Letardi, Appl. Phys. B **47**, 1 (1988).
27. Yu. I. Bychkov, S. L. Gorchakov, and A. G. Yastremskii, Quantum Electron. **30**, 733 (2000).
28. J. L. Lyman, Appl. Opt. **12**, 2736 (1973).
29. C. P. Arnold and R. G. Wenzel, IEEE J. Quantum Electron. **9**, 491 (1973).
30. G. V. Ostrovskaya and A. N. Zaidel, Phys. Lett. A **26**, 393 (1968).
31. G. Kruger, Appl. Opt. **21**, 2841 (1982).
32. S. D. Velikanov, A. S. Elugin, E. A. Kudryashov, I. N. Pegoev, S. N. Sin'kov, and Yu. I. Frolov, Quantum Electron. **27**, 273 (1997).
33. N. A. Vainos, S. Mailis, S. Pissadakis, L. Boutsikaris, P. Dainty, P. J. M. Parmiter, and T. J. Hall, Appl. Opt. **35**, 6304 (1996).

Translated by A. Chikishev